Plasma Phys. Control. Fusion **55** (2013) 014018 (5pp) doi:10.1088/0741-3335/55/1/014018

Self-organized confinement by magnetic dipole: recent results from RT-1 and theoretical modeling

Z Yoshida[1], H Saitoh[1], Y Yano[1], H Mikami[1], N Kasaoka[1], W Sakamoto[1], J Morikawa[1], M Furukawa[1] and S M Mahajan[2]

[1] Graduate School of Frontier Sciences, The University of Tokyo, Chiba 277-8561, Japan
[2] Institute for Fusion Studies, The University of Texas at Austin, Austin, TX 78712, USA

E-mail: yoshida@ppl.k.u-tokyo.ac.jp

Received 30 March 2012, in final form 16 May 2012
Published 17 December 2012
Online at stacks.iop.org/PPCF/55/014018

Abstract
Inhomogeneous magnetic field gives rise to interesting properties of plasmas which are degenerate in homogeneous (or zero) magnetic fields. Magnetospheric plasmas, as observed commonly in the Universe, are the most simple, natural realization of strongly inhomogeneous structures created spontaneously in the vicinity of magnetic dipoles. The RT-1 device produces a 'laboratory magnetosphere' by which stable confinement (particle and energy confinement times $\sim$0.5 s) of high-β (local electron $\beta \sim 0.7$; electron temperature $\gtrsim$10 keV) plasma is achieved. By producing a pure-electron plasma, we obtain clear-cut evidence of inward (or up-hill) diffusion of particles. A statistical mechanical model reveals the 'distortion' of phase space, induced by the inhomogeneity of the ambient magnetic field, on which the plasma relaxes into an equilibrium with inhomogeneous density while it maximizes the entropy.

(Some figures may appear in colour only in the online journal)

1. Introduction

Magnetospheres are self-organized structures found commonly in the Universe. The strong inhomogeneity of a dipole magnetic field gives rise to interesting properties of plasmas which are degenerate in homogeneous (or zero) magnetic fields. We observe spontaneous creation of a steep density gradient toward the higher-magnetic field core region. This naturally produced *confinement* may be applied to various technologies such as advanced fusion [1] and antimatter physics [2]. Apart from these practical purposes, understanding the mechanism that operates beneath this interesting phenomenon is a challenging problem of physics study, which possibly provides us with a new perspective of describing the physics of plasmas.

The aim of this paper is to present an interim summary of the experimental observations and theoretical modeling of the self-organized magnetospheric plasmas. We have constructed a 'laboratory magnetosphere,' the RT-1 device [3] by which we have demonstrated stable confinement (particle and energy confinement times $\sim$0.5 s) of very high-β plasma (local electron beta $\sim$0.7) [4, 5] (the reader is referred to [6, 7] for experiments of similar geometry). Using RT-1, we can also produce a pure-electron non-neutral plasma by injecting electrons from an electron gun placed at the periphery of the confinement region that is bounded by a magnetic separatrix (the dipole confinement of non-neutral plasma [8, 9] is compared with other toroidal systems such as a helical field confinement [10] or a toroidal field confinement [11]). Probing the internal electric field, we have found clear-cut evidence of up-hill diffusion of electrons [12, 13]. Based on these experiments, we postulate that the self-organization is a spontaneous process to vanish a 'free energy' of collective motion by relaxing into an equilibrium state on a *macroscopic scale hierarchy*. A theoretical explanation for the self-organized confinement is given by constructing a distribution function on such a macroscopic scale hierarchy.

This paper is organized as follows: In section 2, we describe the main parameters of the RT-1 device and the experimental observation of 'spontaneous confinement.' In section 3, we present a theoretical model of the self-organization.

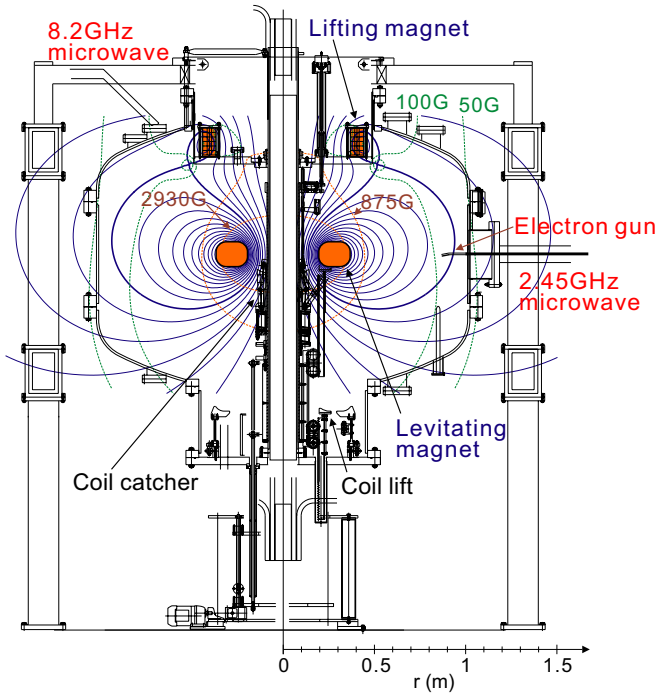

Figure 1. Schematic drawing of the RT-1 device. A dipole magnetic field is produced by the levitating superconducting magnet. A high-β plasma is produced and heated by electron cyclotron heating (ECH) (8.2 and 2.45 GHz). A pure-electron non-neutral plasma is also produced by injecting electrons from an electron gun placed at the periphery of the confinement region (bounded by a magnetic separatrix).

2. Laboratory magnetosphere produced in RT-1

The RT-1 device is a laboratory magnetosphere; levitating a superconducting (Bi-2223 high-T_c superconductor) ring magnet (0.25 MA) in a vacuum chamber (diameter $\sim$2 m), we can produce a magnetospheric plasma (see figure 1). The field strength in the confinement region varies from 0.5 to 0.01 T. The plasma is bounded by a magnetic separatrix that is produced by the lifting magnetic field.

2.1. High-β plasma

High-temperature plasma is produced by electron cyclotron heating (ECH) (8.2 GHz, 25 kW and 2.45 GHz, 20 kW). Electrons consist of hot and cold components; the temperature of the hot component is 10–50 keV, while that of the cold component is typically $\sim$100 eV. The total electron density is of order $10^{17}\,\mathrm{m}^{-3}$. When the filling gas pressure is low ($\lesssim 10^{-3}$ Pa), the cold component is less than 30% of the total electrons [5]. Because of low density and high electron temperature, ions are left cold ($\lesssim$10 eV); direct ion heating by ion cyclotron heating is the main subject of the on-going Phase-II project [14].

By matching solutions of the Grad–Shafranov equation with data from 4-channel flux loops and 14-channel magnetic pickups (as well as an inserted magnetic probe scanning the total range of radius in relatively low-temperature benchmark plasma), we estimate the pressure profile in the plasma; see figure 2. The local β is a strong function of the pressure profile; giving the lowest-possible estimate, we evaluate the local $\beta \sim 0.7$ and the volume average $\beta \sim 0.07$. The high-β confinement is achieved simultaneously with high electron temperature ($\gtrsim$10 keV) and long confinement time (particle and energy confinement times $\sim$0.5 s, which are estimated by the free-decay times after stopping the ECH). The plasma pressure (β) is consistent with the electron temperature and density ($\lesssim 10^{17}\,\mathrm{m}^{-3}$) [4, 5]. The confinement times can be accounted for by classical atomic processes: the ion confinement time is of the same order of the charge-exchange time of ions ($\gtrsim$0.1 s). While hot electrons are decoupled with ions, they couple with the cold electrons with energy equilibration time ($\sim$1 s), and cold electrons are lost with ions by the ambipolar mechanism.

The radial profile of the electron density $n_e(r)$ (measured by 75 GHz microwave interferometry) is highly peaked (giving an indirect proof of the *inward diffusion* of particles [15, 16]; in section 2.2, we give a clear-cut evidence of inward diffusion in a pure-electron non-neutral plasma; the reader is also referred to similar observation in a different experiment [17], as well as discussions on astronomical magnetospheres [18, 19]). Fitting the data by a function $n_e(r) = n_0 r^{-\alpha}$, we estimate $\alpha = 2.8 \pm 0.4$ for a wide range of operating parameters [5]. Multiplying n_e by $\oint \mathrm{d}\ell/B$ ($\mathrm{d}\ell$ is the parallel unit length along the magnetic surface), magnetic-flux tube; see figure 3. While $n_e(r)$ is an increasing function toward the center of the dipole magnetic field, $N_e(r)$ is a decreasing function, hence interchange modes are stable. Note that the simple kinetic model predicts a flat distribution of N_e [15, 16]. The reason why $N_e(r)$ decreases toward the center is explained by the thermodynamic equilibrium model to be described in section 3.

2.2. Pure-electron plasma

RT-1 can also produce a pure-electron plasma by injecting electrons from an electron gun placed at the periphery of the confinement region. A rotating electron cloud (confining typically 10^{-8} C of electrons) sustains stably for more than 300 s [12, 13].

A single-species (non-neutral) plasma has a strong internal electric field. Confinement is possible only if the electric field ($\boldsymbol{E}$) is balanced by an induction ($\boldsymbol{v} \times \boldsymbol{B}$) generated by a vortical motion ($\boldsymbol{v}$) in the magnetic field ($\boldsymbol{B}$). The flow and the electromagnetic field achieve stable coupling by self-organizing a vortex. The non-triviality of *confinement* in the dipole magnetic field may be highlighted by comparing its formation process with that of conventional traps; the most popular method is to inject particles along a straight homogeneous magnetic field and then plug the entrance to the magnetic bottle by applying an electric field. The injected particles form an axisymmetric rigidly rotating column [20, 21]. Magnetospheric non-neutral plasma is produced through an entirely different process. We simply emit electrons from an electron gun placed in a peripheral region of a static dipole magnetic field; we do not need to control the electric or magnetic field. Particles penetrate into the magnetosphere automatically and *self-organize* a stable vortical structure.

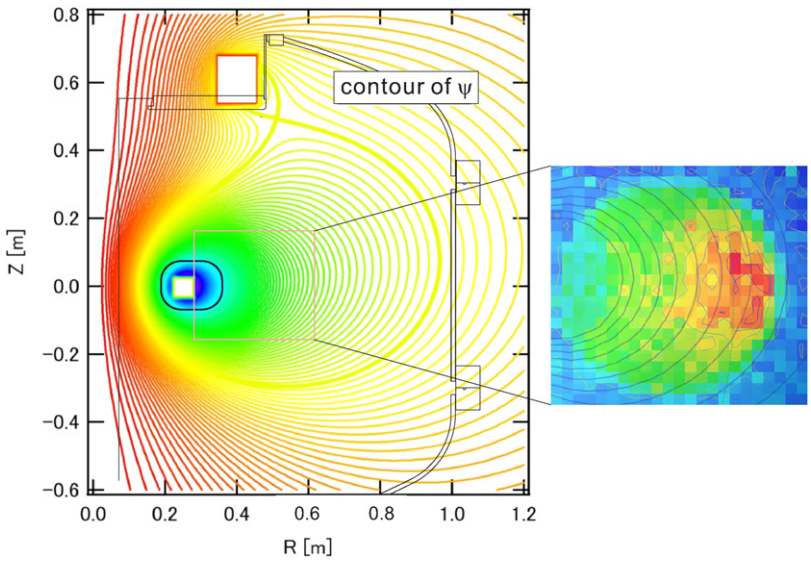

Figure 2. Left: high-β equilibrium reconstructed by a solution of the Grad–Schafranov equation fitting diamagnetic signals. Right: soft-x ray image of the plasma (by auxiliary lines, we show the geometric relation between two plots, but they are from different plasma shots).

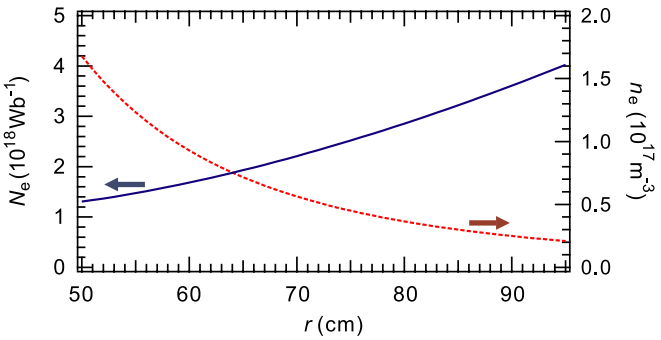

Figure 3. The radial profiles of the electron density n_e, and the electron number N_e per unit flux-tube volume $\oint d\ell/B$ (for the original data, see figure 8 of [5]).

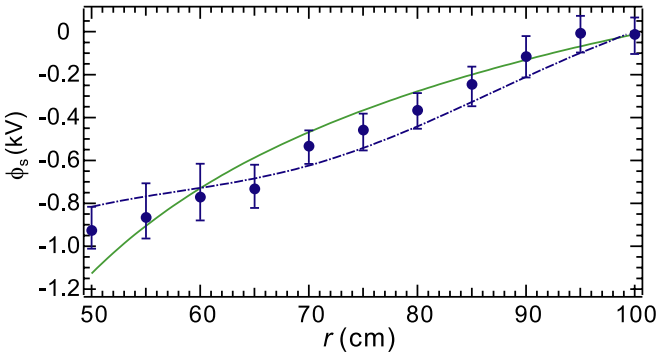

Figure 4. The radial profile of the space potentials inside an electron plasma measure by a high-impedance Langmuir probe (for the original data, see figure 9 of [13]). The solid line shows the space potential profile that corresponds to rigid-rotor $\boldsymbol{E} \times \boldsymbol{B}$ rotation with the observed angular frequency $\omega = 1.9 \times 10^5\,\mathrm{rad\,s^{-1}}$. The electron gun was located at $r = 80\,\mathrm{cm}$ and operated with acceleration voltage 500 V. The chain line is the potential profile calculated from the measured electron density.

The self-organization process is driven by the Kelvin–Helmholtz (or, diocotron) instability, and continues until the plasma establishes a rigidly rotating vortex in which the instability quenches [12]. As shown in figure 4, such a structure is only possible if electrons diffuse inward, climbing up the potential hill—the internal electric potential is higher than the initial kinetic energy (acceleration voltage of the gun) of injected electrons.

3. Theoretical model of dipole confinement

In this section, we describe the self-organized confinement of the dipole configuration as a thermodynamic equilibrium in an effective phase space of magnetized particles which is 'distorted' by the inhomogeneous magnetic field; the maximum entropy equipartition state has an inhomogeneous density when it is immersed in the laboratory flat space.

3.1. Effective Hamiltonian of magnetized particles

We start by reviewing the effective Hamiltonian of a magnetized particle. The Hamiltonian of a charged particle is $H = mv^2/2 + q\phi$, where $\boldsymbol{v} := (\boldsymbol{P} - q\boldsymbol{A})/m$ is the velocity, $\boldsymbol{P}$ is the canonical momentum, $(\phi, \boldsymbol{A})$ is the electromagnetic 4-potential, m (q) is the particle mass (charge). Denoted by $\boldsymbol{v}_\parallel$ and $\boldsymbol{v}_\perp$ the parallel and perpendicular (with respect to the local magnetic field) components of the velocity, respectively we may write

$$H = \frac{m}{2}v_\perp^2 + \frac{m}{2}v_\parallel^2 + q\phi. \tag{1}$$

The velocities are related to the mechanical momentum as $\boldsymbol{p} := m\boldsymbol{v}$, $\boldsymbol{p}_\parallel := m\boldsymbol{v}_\parallel$, and $\boldsymbol{p}_\perp := m\boldsymbol{v}_\perp$. In a strong magnetic field, $\boldsymbol{v}_\perp$ can be decomposed into a small-scale cyclotron motion $\boldsymbol{v}_c$ and a macroscopic guiding-center drift motion $\boldsymbol{v}_d$. The periodic cyclotron motion $\boldsymbol{v}_c$ can be *quantized* to write $mv_c^2/2 = \mu\omega_c(\boldsymbol{x})$ in terms of the magnetic moment μ and the cyclotron frequency $\omega_c(\boldsymbol{x})$; the adiabatic invariant μ and the gyration phase $\vartheta_c := \omega_c t$ constitute an action-angle

pair. For an axisymmetric dipole system with a poloidal (but no toroidal) magnetic field, we define a magnetic coordinate system (ψ, ζ, θ) such that $\boldsymbol{B} = \nabla\psi \times \nabla\theta = B\nabla\zeta$ (θ is the toroidal angle). The macroscopic part of the perpendicular kinetic energy is expressed as $mv_{\rm d}^2/2 = (P_\theta - q\psi)^2/(2mr^2)$, where P_θ is the angular momentum in the θ direction and r is the radius from the geometric axis. In terms of the canonical-variable set $\boldsymbol{z} = (\vartheta_{\rm c}, \mu, \zeta, p_\parallel, \theta, P_\theta)$ the effective Hamiltonian becomes

$$H_{\rm c} = \mu\omega_{\rm c} + \frac{1}{2m}p_\parallel^2 + \frac{1}{2m}\frac{(P_\theta - q\psi)^2}{r^2} + q\phi. \tag{2}$$

The energy of the cyclotron motion has been quantized in terms of the frequency $\omega_{\rm c}(\boldsymbol{x})$ and the action μ; the gyro-phase $\vartheta_{\rm c}$ has been coarse grained (integrated to yield 2π).

The standard Boltzmann distribution function is derived if we assume that $\mathrm{d}^3v\,\mathrm{d}^3x$ is an invariant measure and the Hamiltonian H is the unique determinant of the ensemble. Maximizing the entropy $S = -\int f\log f\mathrm{d}^3v\mathrm{d}^3x$ with constraining the total energy $E = \int Hf\mathrm{d}^3v\mathrm{d}^3x$ and the total particle number $N = \int f\mathrm{d}^3v\mathrm{d}^3x$, we obtain

$$f(\boldsymbol{x}, \boldsymbol{v}) = Z^{-1}\mathrm{e}^{-\beta H}, \tag{3}$$

where Z is the normalization factor. The corresponding configuration-space density

$$\rho(\boldsymbol{x}) = \int f\mathrm{d}^3v \propto \mathrm{e}^{-\beta q\phi}, \tag{4}$$

becomes constant for a charge neutral system ($\phi = 0$).

Needless to say that the Boltzmann distribution or the corresponding configuration-space density, with an appropriate Jacobian multiplication, is independent of the choice of phase-space coordinates. Moreover, the density is invariant no matter whether we quantize the cyclotron morion or not. We confirm this fact by a direct calculation. For the Boltzmann distribution of the 'guiding-center plasma'

$$f(\mu, v_{\rm d}, v_\parallel; \boldsymbol{x}) = Z^{-1}\mathrm{e}^{-\beta H_{\rm c}}, \tag{5}$$

the density is given by

$$\rho(\boldsymbol{x}) = \int f\mathrm{d}^3v = \int f\,\frac{2\pi\omega_{\rm c}}{m}\mathrm{d}\mu\mathrm{d}v_{\rm d}\mathrm{d}v_\parallel \propto \mathrm{e}^{-\beta q\phi}, \tag{6}$$

exactly reproducing (4).

3.2. Effective phase space and distorted metric

What makes the distribution function fundamentally different is the 'constraints' on the phase space which limits the actual domain where the particles can occupy; the adiabatic invariants pose such constraints.

The constancy of the magnetic moment μ imposes the strongest constraint. In addition, the action $J_\parallel$ of the bounce motion (parallel to magnetic field lines) is also an adiabatic invariant that plays an essential role in the strongly inhomogeneous dipole magnetic field. To find explicit expressions for the parallel action-angle variables, we invoke the Hamiltonian $H_{\rm c}$ of (2) in which the gyration action-angle pair μ-$\vartheta_{\rm c}$ is 'quantized' in a sense that $\omega_{\rm c} = \dot{\vartheta}_{\rm c}$ is given as a function of $\boldsymbol{x}$ (configuration-space coordinate). Neglecting the curvature effect and assuming charge neutrality ($\phi = 0$), the equation of the parallel motion reads as

$$m\frac{\mathrm{d}^2}{\mathrm{d}t^2}\zeta = -\mu\nabla_\parallel\omega_{\rm c}. \tag{7}$$

In the vicinity of $\zeta = 0$, where $\omega_{\rm c}$ has a minimum on each magnetic surface, we may expand $\omega_{\rm c} = \Omega_{\rm c}(\psi) + \Omega_{\rm c}''(\psi)\zeta^2/2$, where $\Omega_{\rm c}(\psi)$ is the minimum of $\omega_{\rm c}$ and $\Omega_{\rm c}''(\psi) := \mathrm{d}^2\omega_{\rm c}/\mathrm{d}\zeta^2|_\psi$. In terms of the length $L_\parallel(\psi) := [2\Omega_{\rm c}(\psi)/\Omega_{\rm c}''(\psi)]^{1/2}$, which scales the variation of $\omega_{\rm c}$ along ζ, (7) is integrated to identify the corresponding action-angle variables: $\zeta = \ell_\parallel\sin\vartheta_\parallel$, $\vartheta_\parallel = \omega_{\rm b}t$ with the bounce frequency $\omega_{\rm b} = \sqrt{\Omega_{\rm c}''(\psi)\mu/m} = v_\perp/L_\parallel(\psi)$. The bounce amplitude $\ell_\parallel = [2E_\parallel/(m\omega_{\rm b}^2)]^{1/2}$ is evaluated in terms of the parallel energy $E_\parallel := (mv_\parallel^2)/2|_{\zeta=0} = J_\parallel\omega_{\rm b}$. Assuming $E_\parallel \approx E_\perp := \mu\Omega_{\rm c}$, we estimate $\ell_\parallel \approx L_\parallel$. The action $J_\parallel := \oint mv_\parallel\mathrm{d}\zeta/(2\pi)$ is related to $E_\parallel = J_\parallel\omega_{\rm b}$, and $\mathrm{d}v_\parallel = (\omega_{\rm b}/mv_\parallel)\mathrm{d}J_\parallel = [\omega_{\rm b}/(2mJ_\parallel)]^{1/2}\mathrm{d}J_\parallel$; the latter, using the relation $\omega_{\rm b}/(mv_\parallel) = v_\perp/(L_\parallel mv_\parallel) \approx 1/(mL_\parallel)$, becomes $\mathrm{d}v_\parallel \approx (1/mL_\parallel)\mathrm{d}J_\parallel$.

The equilibrium distribution function is derived by maximizing entropy S over a micro-canonical ensemble of a given particle number N, an energy E, a total magnetic moment $M_{\rm c} = \int\mu f\mathrm{d}^6z$ and a total bounce action $M_{\rm b} = \int J_\parallel f\mathrm{d}^6z$:

$$f_{\alpha,\gamma} = Z^{-1}\mathrm{e}^{-(\beta H_{\rm c} + \alpha\mu + \gamma J_\parallel)}, \tag{8}$$

where β, α, γ and $\log Z - 1$ are, respectively, the Lagrange multipliers on E, $M_{\rm c}$, $M_{\rm b}$, and N. Or, interpreting this $f_{\alpha,\gamma}$ as a distribution function of a grand-canonical ensemble, β is the inverse temperature, α/β and γ/β are the *chemical potentials* associated with the quasi-particles carrying microscopic actions μ and $J_\parallel$.

The corresponding coordinate-space density is

$$\begin{aligned}\rho &= \int f_{\alpha,\gamma}\,\frac{2\pi\omega_{\rm c}\mathrm{d}\mu}{m}\frac{\mathrm{d}J_\parallel}{mL_\parallel(\psi)}\mathrm{d}v_{\rm d} \\ &\propto \frac{\omega_{\rm c}(\boldsymbol{x})}{m^2}\int_0^\infty \frac{\mathrm{e}^{-(\beta\omega_{\rm c}+\alpha)\mu}\mathrm{d}\mu}{\beta\sqrt{2\omega_{\rm c}\mu/m} + \gamma L_\parallel(\psi)}.\end{aligned} \tag{9}$$

Note that the Jacobian weight $\propto \omega_{\rm c}/L_\parallel(\psi)$, representing the distortion of the metric on the constrained effective phase space, introduces a coordinate-space inhomogeneity; see figure 5. As shown in figure 3, the electron density is strongly peaked in the laboratory frame, but is hollow when multiplied by the flux-tube volume $\oint\mathrm{d}\ell/B \propto \overline{L_\parallel/\omega_{\rm c}}$ ($\overline{x}$ denotes the orbit average of x)—the decrease in the core (high $\omega_{\rm c}$) region, avoiding the divergence in the limit of the flux-tube volume $\to 0$, is due to the Boltzmann factor $\mathrm{e}^{-\beta\omega_{\rm c}\mu}$ with a finite temperature β^{-1} (which was omitted in previous models).

4. Summary

We have obtained experimental proof of the *self-organization* and *inward diffusion* in plasmas (both high-temperature, quasi-neutral and pure electron, non-neutral) which are

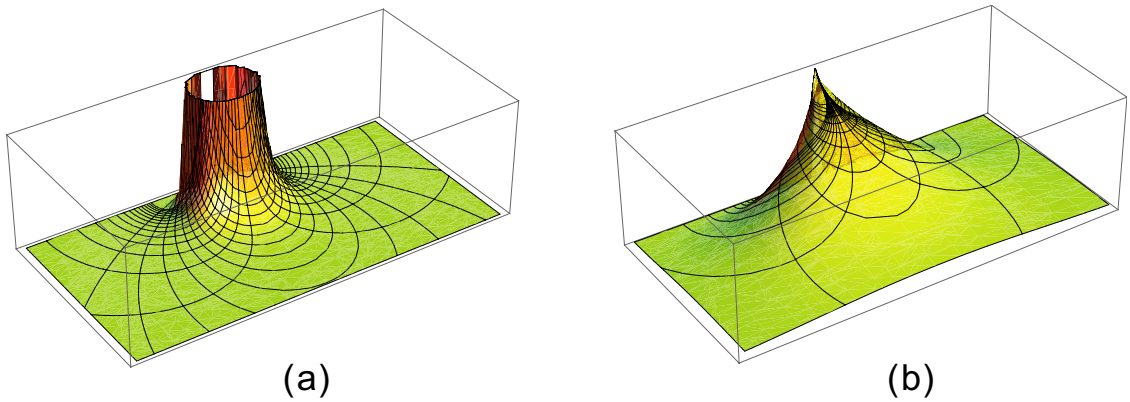

Figure 5. (*a*) Distorted coordinate-space metric (equivalent to the reciprocal flux-tube volume) in a dipole magnetic field. (*b*) Thermodynamic equilibrium on the constrained phase space; by immersing in the laboratory flat space, we obtain a heterogeneous density distribution.

spontaneously confined in a dipole magnetic field. The creation of a strongly localized density profile is explained by *distortion* of the metric on the effective (or, macroscopic) phase space; the maximum-entropy, equipartition distribution on the distorted phase space has inhomogeneous density when it is immersed in the laboratory flat space.

Acknowledgments

The authors are grateful to Professor Akira Hasegawa for useful discussions. This work was supported by Grant-in-Aid for Scientific Research from the Japanese Ministry of Education, Science and Culture No 23224014.

References

[1] Hasegawa A *et al* 1990 *Nucl. Fusion* **30** 2405
[2] Yoshida Z *et al* 1999 *Non-neutral plasma physics III AIP Conf. Proc.* **498** 397
[3] Yoshida Z *et al* 2006 *Plasma Fusion Res.* **1** 008
[4] Saitoh H *et al* 2011 *Phys. Plasmas* **18** 056102
[5] Saitoh H *et al* 2011 *Nucl. Fusion* **51** 063034
[6] Mauel M, Warrren H and Hasegaw A 1992 *IEEE Trans. Plasma Sci.* **20** 626
[7] Garnier D T *et al* 2006 *Phys. Plasmas* **13** 056111
[8] Kondoh S and Yoshida Z 1996 *Nucl. Instrum. Methods Phys. Res.* A **382** 561
[9] Saitoh H *et al* 2004 *Phys. Rev. Lett.* **92** 255005
[10] Kremer J P *et al* 2006 *Phys. Rev. Lett.* **97** 095003
[11] Marler J P and Stoneking M R 2008 *Phys. Rev. Lett.* **100** 155001
[12] Yoshida Z *et al* 2010 *Phys. Rev. Lett.* **104** 235004
[13] Saitoh H *et al* 2010 *Phys. Plasmas* **17** 112111
[14] Yoshida Z *et al* 2010 *Phys. Plasmas* **17** 112507
[15] Hasegawa A 1987 *Comment. Plasma Phys. Control. Fusion* **11** 147
[16] Hasegawa A 2005 *Phys. Scr.* **T116** 72
[17] Boxer A C *et al* 2010 *Nature Phys.* **6** 207
[18] Schulz M and Lanzerotti L J 1974 *Particle Diffusion in the Radiation Belts* (New York: Springer)
[19] Chen Y, Reeves G D and Friedel R H W 2007 *Nature Phys.* **3** 614
[20] Dubin D H E and O'Neil T M 1999 *Rev. Mod. Phys.* **71** 87
[21] O'Neil T M 1999 *Phys. Today* **52** 24